Journal of Saudi Chemical Society (2015) **xxx**, xxx–xxx

King Saud University

Journal of Saudi Chemical Society

www.ksu.edu.sa
www.sciencedirect.com

ORIGINAL ARTICLE

Synthesis and characterization of azomethine polymers containing ether and ester groups

Dilek Şenol *, **İsmet Kaya** *

Çanakkale Onsekiz Mart University, Department of Chemistry, Polymer Synthesis and Analysis Lab., 17020 Çanakkale, Turkey

Received 7 February 2015; revised 8 May 2015; accepted 10 May 2015

KEYWORDS

Azomethine polymers;
Synthesis;
Thermal analysis;
Emission spectra

Abstract In this study, Schiff base was synthesized from the reaction of 4-carboxybenzaldehyde and 4-amino-3-methyl. Then, the obtained Schiff base was acted with aromatic and aliphatic dihalogen compounds in argon environment, and the polymers containing both ester and ether groups were obtained. For the structural analyses of synthesized substances FT-IR and NMR analysis, for the optical properties fluorescence and UV–Vis measurements, and for the thermal analyses TG-DTA and DSC techniques were used. In addition, electrochemical and electrical conductivity measurements were carried out. Aromatic imine polymers and their derivatives were already synthesized, and the properties such as high thermal resistance, low band gap and semi-conductive properties were also described in literature. In this study, new kinds of polymers synthesized are expected to have a high thermal resistance with elastic aliphatic and conjugated aromatic groups. The effects of the presence of etheric bonds and ester groups in the main chain of the polymers on several physical and thermal properties are also aimed to be explored.

1. Introduction

Conjugated aromatic poly(azomethine)s (or polyimines) can also be used in several areas due to their semi-conductive properties. In addition, azomethine Schiff base polymers derived from *ortho*-hydroxy aromatic aldehydes many times can form stable chelate polymers with transition metals and can be used as ion sensors by utilizing such properties. Since conjugated poly(azomethine)s have fluorescence properties, they can be used in the manufacturing of polymer light-emitting diodes (PLED) [1].

It is known that conjugated poly(azomethine)s are used in the manufacturing of electro-chromic materials constituting the basis of LCD display technology and in solar cells [2]. Polyester is an important class of the polymer world and makes human life easier by being used in textile, automobile, pharmacology, biomedical devices, surgical equipment, coating industry, structural engineering, electronic device applications etc. in daily life. Poly(azomethine-ester)s in polyester and polyazomethine class have a considerably high thermal resistance, exhibit semi-crystalline behaviors in different mesophases and have a high optical transmittance [3–7].

* Corresponding authors. Fax: +90 286 218 05 33.
E-mail addresses: dilek_dilek1734@hotmail.com (D. Şenol), kayaismet@hotmail.com (İ. Kaya).

Peer review under responsibility of King Saud University.

ELSEVIER Production and hosting by Elsevier

http://dx.doi.org/10.1016/j.jscs.2015.05.006

Please cite this article in press as: D. Şenol, İ. Kaya, Synthesis and characterization of azomethine polymers containing ether and ester groups, Journal of Saudi Chemical Society (2015), http://dx.doi.org/10.1016/j.jscs.2015.05.006

In a study conducted by He et al. [8], a new polymer containing a bithiazole ring was synthesized and the polyester was characterized by FT-IR spectroscopy, elemental analysis and X-ray diffraction spectroscopy. Thermal decomposition of the polyester in nitrogen atmosphere was discussed with thermogravimetric analyses. Activation energy in decomposition step of the polyester was calculated by using iso-conventional method. At the end of the analyses, it was found that polyester had an amorphous structure, its softening temperature was 503.9 K and average mass loss was 60% [8]. In a study conducted by Iwan et al. [9], the synthesized polyesters were characterized by FT-IR, ^{1}H, ^{13}C NMR spectrometers and elemental analysis, and their ability to form a thin film on quartz substrate with their UV–Vis properties was discussed. Thermo-luminescence properties were examined at various temperatures between 25 and 200 °C. Mesomorphic behaviors of polyesters were investigated by using DSC and POM (Polarized optical micrographs) techniques. ITO/PEDOT/PAZ:TiO_2/Al structures were discussed with BHJ electrical and layered characterization methods. The electrical behaviors at different temperatures were investigated by using Impedance spectroscopy. The local intensities and phases on the surface were explained with AFM images. It was detected that polyazomethines with optoelectronic properties and all other polyesters with semi-conductive properties in their thin films were observed. In consideration of these findings, polyesters were thought to be a good candidate for the design of optoelectronic devices and solar cells [9].

By considering these properties, in this study, it was aimed to determine the change of thermal, fluorescence and morphologic properties of poly(azomethine-ester)s with dihalogens attached to the main chain which were synthesized by the ester and etheric groups. Structural characterization of the synthesized Schiff base and poly(azomethine-ester) derivatives was carried out by using FT-IR, ^{1}H NMR, ^{13}C NMR and SEC techniques. Optical properties of the prepared Schiff bases and polyester derivatives containing azomethine bond were revealed by using UV–Vis spectroscopy. Electrochemical properties of the obtained compounds were explained by using cyclic voltammetry (CV) technique. Thermal stabilities of the synthesized Schiff base and its polyester derivatives were examined by using TG-DTA and DSC devices. Morphologic properties of the synthesized polyesters containing azomethine bond were explained by SEM device.

2. Materials and method

2.1. Materials

While all solvents and chemicals were provided from Merck (Germany) Company, only sodium hypochlorite (30%) was purchased from Paksoy Chemicals Company. They are used in experiments without the need of initial purification.

2.2. Solubility of the compounds

Solubility tests of the synthesized polymers were carried out in several solvents by using 1 mg of sample and 1 mL solvent. The polymers were dissolved well in solvents like ethanol, methanol, chloroform, acetone, acetonitrile, tetrahydrofuran (THF), dimethylformamide (DMF) and dimethylsulfoxide (DMSO). It was observed that they did not dissolve in apolar solvents like benzene, heptane, ethyl acetate etc. The presence of an oxygen atom and a flexible aliphatic group along the polymer chain increased the solubility of the polymer [10].

2.3. Monomer synthesis

At first, Schiff base monomer was synthesized by a condensation reaction using aromatic amine and aromatic aldehyde (Scheme 1). In order to carry out the reaction, first of all 2-amino-5-methyl phenol (2A5MP) (2 g, 0.013 mol) was weighed and put into a 250 mL three-neck, round bottom reaction flask, and then 30 mL of methanol was added and it was dissolved at room temperature by continuous mixing on a hot plate magnetic stirrer under condenser. Then, an aldehyde compound, 4-carboxybenzaldehyde (4CBA) (1.64 g, 0.013 mol) dissolved in 30 mL of methanol was added into the reaction flask, and was let to form a Schiff base monomer at room temperature. A dark yellow Schiff base, CBAAMP was poured into a petri dish. The solvent was allowed to evaporate by leaving the petri dish open. The precipitated products were crystallized by acetonitrile.

CBAAMP: ^{1}H NMR (DMSO-d_6): δ ppm, 10.07 (s, 1H, —COOH), 9.04 (s, 1H, —OH), 8.78 (s, 1H, —CH=N), 8.11 (d, 2H, Ar-He), 8.03 (d, 2H, Ar-Hd), 7.17 (d, 1H, Ar-Hc), 6.72 (s, 1H, Ar-Ha), 6.64 (d, 1H, Ar-Hb), 2.22 (s, 3H, —CH_3). CBAAMP: ^{13}C NMR (DMSO-d_6): δ ppm, 167.0 (C13-H), 156.73 (C8-H), 151.61 (C1-H), 140.24 (C12-ipso), 137.88 (C7-ipso), 134.52 (C9-ipso), 132.50 (C3-ipso), 129.52 (C11-H), 128.70 (C10-H), 120.22 (C6-H), 118.77 (C5-H).

2.4. Polymer synthesis

Four different types of polymers were synthesized by carrying out an esterification reaction between the synthesized monomer and various aliphatic and aromatic dihalogen compounds and they are shown in Scheme 2. The synthesis of polymer was carried out as follows: 1 g (3.92×10^{-3} mol) of CBAAMP monomer dissolved in 30 mL of *N*,*N*-dimethylformamide (DMF) was put into a 250 mL three-neck, round bottom reaction flask with a magnetic stirrer and the reaction was heated up to 180 °C under condenser and argon gas. Then 0.4 g of Na_2CO_3 was added into the reaction flask, and —OH and —COOH groups in the monomer were allowed to be converted into salt for 30 min. After this process, the dihalogen compound, *p*-xylenedibromide (XB) (1.15 g, 4.2×10^{-3} mol) dissolved in 10 mL of DMF was added into the reaction medium, and the reaction was kept at 180 °C under argon gas for 8 h. For other three different dihalogens compounds, 1,12-dibromododecane (BD) (0.52 g, 4.3×10^{-3} mol), 2-chloroethylether (CEE) (0.64 g, 4.4×10^{-3} mol) and 1,2-bis(2-chloroethoxy)ethane

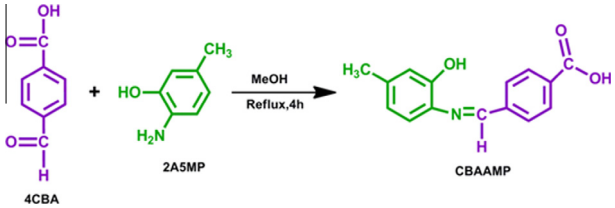

Scheme 1 Syntheses of the CBAAMP monomer.

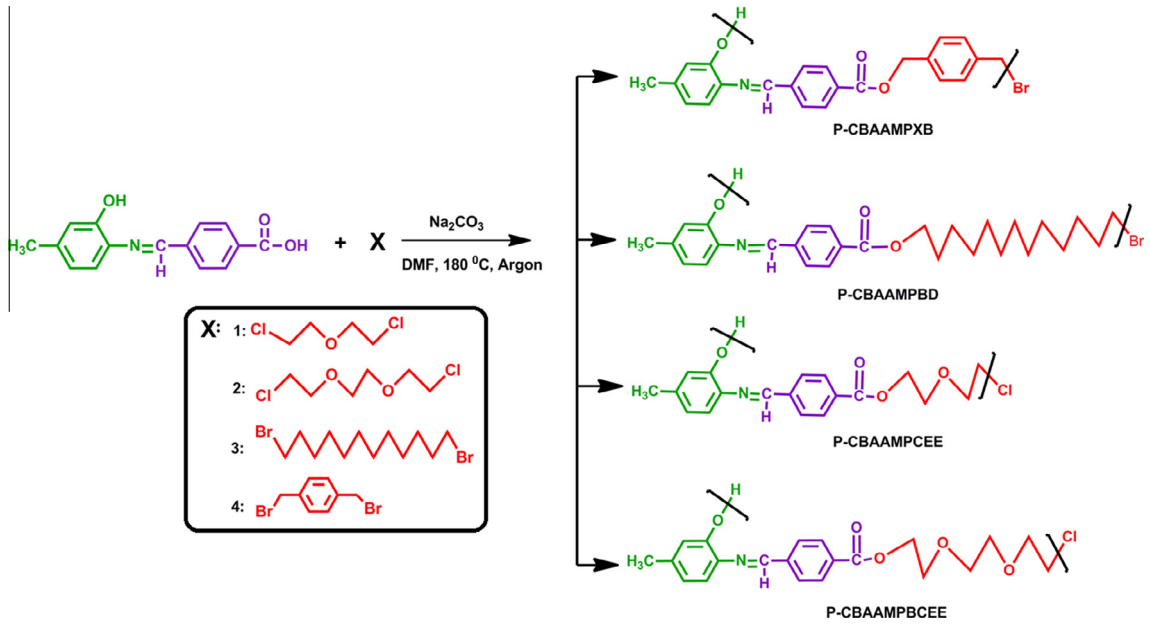

Scheme 2 Syntheses of the polymers.

(BCEE) (0.82 g, 4.3×10^{-3} mol), the same apparatus was set up, and they were added into the reaction environment under same conditions and dark brown-black polymers were obtained at the end of the reaction.

The mixtures cooled down after the reaction was precipitated by being poured into beakers containing 250 mL of water. The precipitation on time was ensured by controlling the P^H by adding ice or 10% HCl if necessary. The synthesized polymer was separated from the medium by filtering, but the salt was removed by thoroughly washing the filter paper. Among these polymers, the polymer including 1,2-bis(2-chloroethoxy)ethane and 2-chloroethylether containing ether group did not precipitate in iced water and acid, they were removed by carrying out extraction with dichloromethane. As a result, more viscous polymers were obtained due to the presence of etheric groups. They were dried in vacuum drying-oven for 24 h.

Elemental analysis results: P-CBAAMPXB: Calc. (Found) C; 77.31 (73.35), H; 5.32 (1.99), N; 3.92 (3.81). P-CBAAMPXB: Calc. (Found) C; 77.31 (73.35), H; 5.32 (1.99), N; 3.92 (3.81). P-CBAAMPBD: Calc. (Found) C; 77.24 (71.05), H; 8.50 (2.74), N; 3.21 (4.25). P-CBAAMPCEE: Calc. (Found) C; 70.15 (64.57), H; 5.84 (2.70), N; 4.30 (4.60). P-CBAAMPBCEE: Calc. (Found) C; 68.29 (67.50), H; 6.23 (2.13), N; 3.79 (4.84).

P-CBAAMPXB: ^{1}H NMR (DMSO-d_6): δ ppm, 10.04 (s, 1H, —CH═N), 8.17 (s, 2H, Ar-He), 7.89 (s, 2H, Ar-Hd), 7.48 (m, 4H, Ar-Hi, Ar-Hj), 7.14 (s, 1H, Ar-Hc), 6.78 (s, 1H, Ar-Ha), 6.56 (s, 1H, Ar-Hb), 5.39 (s, 1H, Ar-Hf), 4.69 (s, 1H, Ar-Hk), 2.47 (s,3H, —CH_3). P-CBAAMPXB: ^{13}C NMR (DMSO-d_6): δ ppm, 191.70 (C13-ipso), 165.33 (C8-H), 154.19 (C1-ipso), 142.55 (C9-ipso), 139.13 (C3-ipso), 136.44 (C7-ipso), 135.85 (C15-ipso, C18-ipso), 134.88 (C12-ipso), 130.27 (C11-2H), 129.52 (C10-2H), 128.63 (C17-2H), 127.30 (C16-2H), 122.15 (C6-H), 119.58 (C5-H), 110.02 (C2-H), 68.87 (C14-2H), 35.31 (C19-2H), 21.79 (C4-3H). P-CBAAMPBD: ^{1}H NMR (DMSO-d_6): δ ppm, 10.09 (s, 1H, —CH═N), 8.15 (d, 2H, Ar-He), 7.95 (d, 2H, Ar-Hd), 7.27 (d, 1H, Ar-Hc), 6.86 (s, 1H, Ar-Ha), 6.70 (d, 1H, Ar-Hb), 4.35 (s, 2H, Ar-Hf), 2.52 (s,3H, —CH_3). 2.82 (s, 4H, Ar-Hk), 1.78 (s, 4H, Ar-Hm, Ar-Hg), 1.43 (s, 2H, Ar-Hi), 1.29 (s, 12H, Ar-Hj, Ar-Hk). P-CBAAMPBD: ^{13}C NMR (DMSO-d_6): δ ppm, 191.73 (C3-ipso), 165.98 (C8-H), 151.11 (C1-ipso), 139.02 (C12-ipso), 136.35 (C7-ipso), 135.46 (C9-ipso), 132.65 (C3-ipso), 130.13 (C11-2H), 129.50 (C10-2H), 121.33 (C6-H), 119.60 (C5-H), 116.22 (C2-H), 77.34 (C1-ipso), 65.80 (C14-ipso), 34.88 (C22-2H), 32.65 (C21-2H), 30.30 (C15-2H), 29.46 (C17-2H, C18-2H), 28.62 (C19-2H), 25.99 (C16-2H), 21.87 (C4-3H). P-CBAAMPCEE: ^{1}H NMR (DMSO-d_6): δ ppm, 10.04 (s, 1H, —CH═N), 8.15 (d, 2H, Ar-He), 7.93 (d, 2H, Ar-Hd), 7.40 (s, 1H, Ar-Hc), 7.27 (s, 1H, Ar-Ha), 6.83 (d, 1H, Ar-Hb), 4.53 (s, 2H, Ar-Hf), 3.88 (s, 2H, Ar-Hg), 3.66 (s, 2H, Ar-Hi), 2.51 (s, 3H, —CH_3). P-CBAAMPBCEE: ^{1}H NMR (DMSO-d_6): δ ppm, 10.05 (s, 1H, —CH═N), 8.15 (d, 2H, Ar-He), 7.92 (d, 2H, Ar-Hd), 7.40 (s, 1H, Ar-Hc), 7.27 (s, 1H, Ar-Ha), 6.83 (d, 1H, Ar-Hb), 4.50 (s, 2H, Ar-Hf), 3.86 (s, 4H, Ar-Hg), 3.70 (s, 4H, Ar-Hi), 3.62 (s,2H, Ar-Hj), 2.51 (s, 3H, —CH_3).

P-CBAAMPBCEE: ^{13}C NMR (DMSO-d_6): δ ppm,191.67 (C13-ipso), 161.40 (C8-H), 151.10 (C1-ipso), 139.68 (C9-ipso), 136.38 (C3-ipso), 134.35 (C7-ipso), 132.17 (C12-ipso), 130.18 (C11-2H), 127.26 (C10-2H), 121.13 (C6-1H), 119.60 (C5-1H), 115.76 (C2-H), 71.39 (C16-2H), 70.65 (C15-2H, C18-2H), 69.20 (C17-2H), 64.40 (C14-2H), 42.76 (C19-2H), 21.88 (C4-3H).

2.5. Characterization techniques

The solubility tests were done in different solvents by using 1 mg sample and 1 mL solvent at 25 °C. The infrared and ultraviolet–visible spectra were measured by PerkinElmer FT-IR Spectrum one and by Analytik jena Specord 210 Plus, respectively. The FT-IR spectra were recorded using universal ATR sampling accessory (4000–550 cm^{-1}). ^{1}H and ^{13}C NMR spectra

(Bruker AC FT-NMR spectrometer operating at 400 and 100.6 MHz, respectively) were also recorded by using deuterated DMSO-d_6 as a solvent at 25 °C. Tetramethylsilane was used as internal standard. Thermal data were obtained by using a PerkinElmer Diamond Thermal Analysis system. TG-DTA measurements were made between 10 and 1000 °C (in N_2, rate 10 °C/min). DSC analyses were carried out by using PerkinElmer Pyris Sapphire DSC. DSC measurements were made between 25 and 420 °C (in N_2, rate 10 °C/min). The number average molecular weight (M_n), weight average molecular weight (M_w) and polydispersity index (PDI) were determined by Gel Permeation Chromatography-Light Scattering (GPC-LS) device of Malvern Viscotek GPC Dual 270 max. For GPC investigations a medium 300 × 8.00 mm Dual column was used. Additional 1 g/L of lithium bromide in DMF (1 mL/min) was used as solvent. Light Scattering Detector (LS) and a refractive index detector (RID) were used to analyze the products at 55 °C. Elemental analyses of compounds were carried out by a CHNS – (Costech ECS 4010) analyzer.

2.6. Optical and electrochemical properties

Ultraviolet–visible (UV–Vis) spectra were measured by Analytik jena Specord 210 Plus. The absorption spectra were recorded by using DMSO at 25 °C. The optical band gaps (E_g) were calculated from their absorption edges.

Cyclic voltammetry (CV) measurements were carried out with a CHI 660 C Electrochemical Analyzer (CH Instruments, Texas, USA) at a potential scan rate of 20 mV/s. All the experiments were performed in a dry box filled with argon at room temperature. The electrochemical potential of Ag was calibrated with respect to the ferrocene/-ferrocenium (Fc/Fc^+) couple. The half-wave potential ($E^{1/2}$) of (Fc/Fc^+) was measured in acetonitrile solution of 0.1 M tetrabutylammonium hexafluorophosphate ($TBAPF_6$) and was 0.39 V with respect to Ag wire. Voltammetric measurements were carried out in acetonitrile for Schiff bases and acetonitrile/DMSO mixture (v/v:5/1) for polymers.

2.7. Electrical properties

Conductivities of the synthesized materials were measured on a Keithley 2400 Electrometer. The pellets were pressed on a hydraulic press developing up to 1687.2 kg/cm^2. Iodine doping was carried out by exposure of the pellets to iodine vapor at atmospheric pressure and room temperature in desiccators. Measurements were carried out per 24 h [11,12].

2.8. Fluorescence measurements

A Shimadzu RF-5301PC spectrofluorophotometer was used in fluorescence measurements. Emission and excitation spectra of the synthesized compounds were obtained in solution forms in DMF for monomers and polymers. Measurements were made in a wide concentration range between 3.125 and 100 mg/L to determine the optimal fluorescence concentrations. Slit width in all measurements was 5 nm.

3. Results and discussion

3.1. Spectral analyses of the synthesized compounds

Structures of the synthesized monomer and polymers were explained with FT-IR, UV–Vis, ^{1}H NMR and ^{13}C NMR analyses. Spectrums were taken by using Fourier Transform Infrared (FT-IR) Spectrometer (Perkin Elmer FT-IR Spectrum one, with ATR sampling accessory). In spectrum

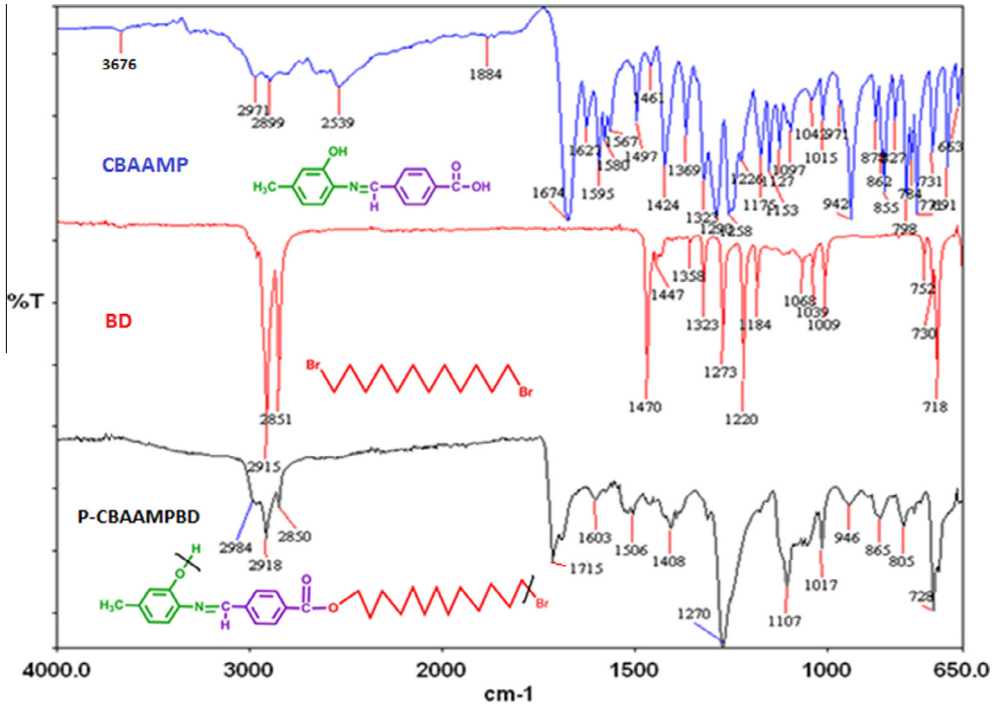

Figure 1 FT-IR spectrum of the polymer synthesized in the presence of 1,12-dibromododecane of monomer.

Table 1 FT-IR spectral data of the synthesized compounds.

Functional groups (cm^{-1})	Compounds			
	CBAAMP	P-CBAAMPXB	P-CBAAMPBCEE	P-CBAAMPCEE
—OH	3676	–	–	–
C—H (aromatic)	3050	3040	3045	3030
C—H (aliphatic)	2971	2960	2948	2964
	2899	2868	2870	2865
C═O (aldehyde and acid)	1674	–	–	–
—C═N	1627	1599	1598	1600
C═C	1595	1578	1523	1519
C—O—C(oxyphenylene)	–	1098	1100	1103
C—OH(phenylene)	–	1260	1268	1266
R—C═O—OR′	–	1713	1715	1718

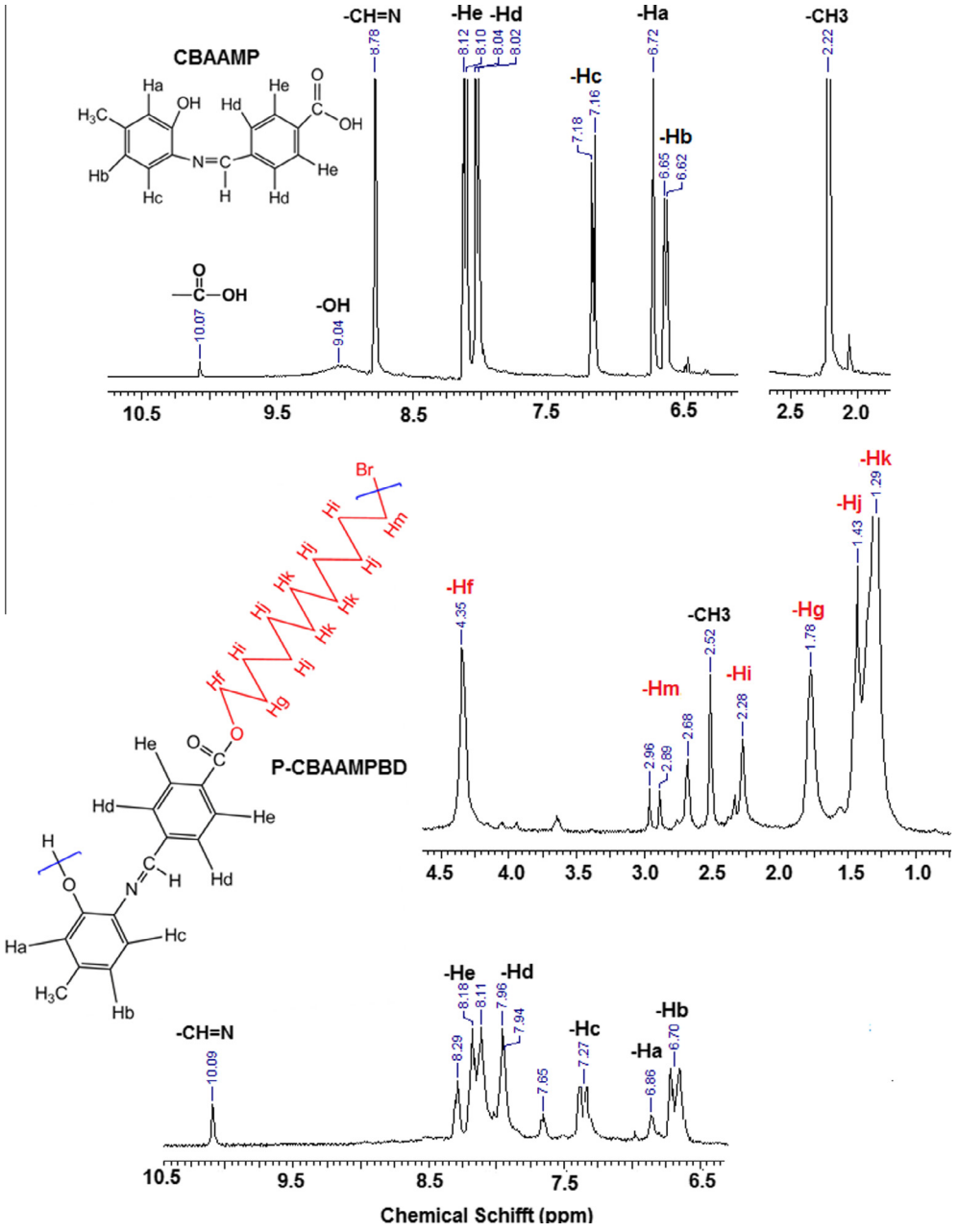

Figure 2 ^{1}H NMR spectra of CBAAMP and P-CBAAMPBD.

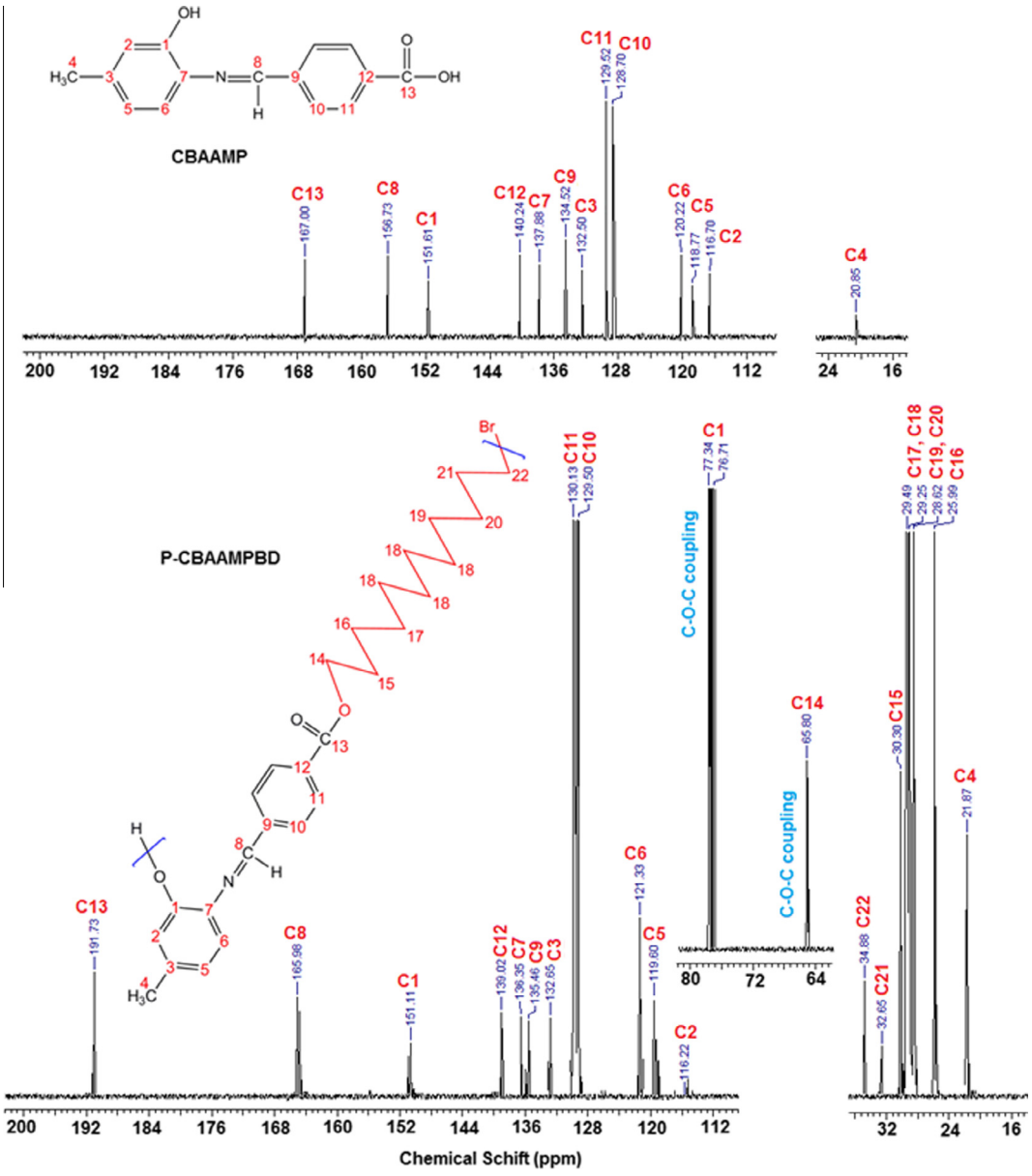

Figure 3 ^{13}C NMR spectra of CBAAMP and P-CBAAMPBD.

Table 2 The number average molecular weight (M_n), weight average molecular weight (M_w), polydispersity index (PDI) of the synthesized polymers.

Compounds	M_n	M_w	PDI	RI Area (mv/mL)	RALS Area (mv/mL)	LALS Area (mv/mL)	Sample Conc. (mg/mL)	dn/dc (mL/g)
P-CBAAMPXB	72.420	132.200	1.826	119.47	220.41	141.05	10.750	0.1032
P-CBAAMPBD	51.380	118.160	2.300	121.72	187.49	115.17	11.800	0.0958
P-CBAAMPBCEE	32.140	73.180	2.277	147.58	180.23	110.29	11.150	0.1229
P-CBAAMPCEE	21.160	45.130	2.133	6.27	87.37	54.97	5.000	0.0116

RI: refractive index, RALS: Right Angle Light Scattering (90 °C), LALS: Low Angle Light Scattering (7 °C).

of the monomer, the expected peak of acid and aldehyde carbonyl belonging to 4-carboxybenzaldehyde (4CBA) involved the peak of aldehyde at 1679 cm^{-1} and was broader than expected and caused the carbonyl peak of aldehyde to disappear. In addition to this, —CH tension belonging to aldehyde at 2951 and 2828 cm^{-1} for 4CBA was observed. The double peaks of amine at 3371 and 3283 cm^{-1} are observed for 2-amino-5-methyl phenol (2A5MP). In spectrum

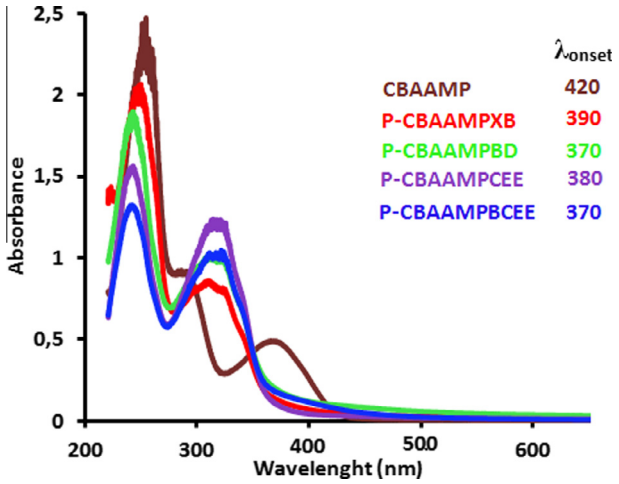

Figure 4 Absorption spectra of the synthesized compounds.

given in Fig. 1, for Schiff base monomer (CBAAMP) —OH peak at 2A5MP was observed at 3676 cm^{-1} and —OH (hydroxyl) and C═O (carbonyl) peaks of acid in 4CBA were observed at 2971–2899 cm^{-1} and 1674 cm^{-1}, respectively. The transition of NH_2 groups into imine (—HC═N) group by undergoing condensation was observed at 1627 cm^{-1}. In spectrum given in Fig. 1, polymer (P-CBAAMPBD) which was formed as a result of reaction between 1,12-dibromododecane dihalogens (BD) and CBAAMP monomer was shown. Accordingly, peaks of the groups of C—O—C(oxyphenylene) at 1107 cm^{-1} and C—OH (phenylene) at 1270 cm^{-1} proved that the —OH peak of the monomer at 3676 cm^{-1} disappeared as a result of polymer formation. Ester carbonyl formed as a result of esterification reaction of the —COOH group was seen at 1715 cm^{-1}. While the aliphatic —CH stretching peaks of 1,12-dibromododecane were sharply seen at 2915 and 2851 cm^{-1}, the same peaks were observed at 2918 and 2850 cm^{-1} for the polymer. It was observed that the imine bond in CBAAMP monomer at 1627 cm^{-1} shifted to 1603 cm^{-1} in P-CBAAMPBD polymer. The functional group peak values of other polymers are given in Table 1.

^{1}H NMR and ^{13}C NMR spectrums of monomers and polymers were taken at DMSO-d_6. The structures, the marking of protons and the chemical shifts of ^{1}H NMR and ^{13}C NMR of monomer, CBAAMP and its polymer, P-CBAAMPBD are given in Figs. 2 and 3. ^{1}H NMR spectrum of CBAAMP monomer gives sharp proton signals as expected, but the acidic proton was not observed since the volatile hydrogen of carboxylic acid and deuteron DMSO hydrogen were interchanged. The hydroxyl, azomethine and aromatic proton signals were observed in 10.07, 8.78 and 8.12–6.82 ppm range, respectively. In ^{1}H NMR spectrum of polymers, an increase in the number of the peaks and an enlargement of the peaks were observed. This enlargement is caused by the presence of repeated monomer units with different chemical environments. The disappearance of both hydroxyl peaks of carboxylic and phenol groups in the polymer indicates that polymerization went through the esterification reaction and the etheric bridge. According to the ^{13}C NMR spectrum of the monomer and polymer, it was observed that the peak seen at 167 ppm shifted to 190 ppm. Oxyphenylene (C—O—C) carbon signals formed due to the attachment were observed at 73.34, 76.71 and 65.80. Nine different carbon signals of CH_2 groups which were involved in the structure were observed between 34.88 and 21.87.

The average molar weights of synthesized are given in Table 2. The molar masses values of polymers are changed between 45.130 and 132.200 g mol^{-1}. According to the average molecular weight, the number of repeating units in P-CBAAMPXB, P-CBAAMPBD, P-CBAAMPBCEE and P-CBAAMPCEE are 254, 315, 165 and 113, respectively. While the molar mass increases, the observation of amorphous structure due to deformations in the regular structure of polymer is higher [13].

When UV spectrum given in Fig. 4 is examined, the absorption peaks of $\pi \rightarrow \pi^*$ electronic transitions of the aromatic ring at 253 nm for the monomer can be seen. In polymer, it is observed that this peak shifted to the left due to halogen ions attached to the main structure and etheric bridge. For

Table 3 Electronic structure parameters of the synthesized compounds.

Compounds	E_{ox} (mV)	E_{Red} (mV)	[a]HOMO (eV)	[b]LUMO (eV)	[c]E'_g (eV)	[d]E_g (eV)
CBAAMP	1254	−818	−5.64	−3.57	2.07	2.95
		−1142		−3.25	2.39	
		−1507		−2.88	2.76	
P-CBAAMPXB	1324	−1260	−5.71	−3.13	2.58	3.18
		−1453		−2.94	2.77	
P-CBAAMPBD	1267	−1200	−5.66	−3.19	2.47	3.35
		−1484		−2.91	2.75	
P-CBAAMPBCEE	1400	−1236	−5.79	−3.15	2.64	3.35
		−1498		−2.89	2.90	
P-CBAAMPCEE	1418	−1245	−5.81	−3.14	2.67	3.27
		−1511		−2.88	2.93	

[a] Highest occupied molecular orbital.
[b] Lowest unoccupied molecular orbital.
[c] Electro optical band gap.
[d] Optical band gap.

P-CBAAMPXB, P-CBAAMPBD, P-CBAAMPCEE and P-CBAAMPBCEE, $\pi \rightarrow \pi^*$ is 248, 242, 242 and 241 nm respectively. While the peak at 370 nm observed in the monomer indicates $n \rightarrow \pi^*$ transition of the azomethine group, this transition is observed for P-CBAAMPXB, P-CBAAMPBD, P-CBAAMPCEE and P-CBAAMPBCEE $n \rightarrow \pi^*$ 310, 314, 318 and 317 nm, respectively. The effect of functional groups incorporation into the polymer backbone, on the optical properties was tested. The introduction of different dihalogen groups as in polyester in comparison with monomer resulted in a hypsochromic shift of the λ_{max} band from 420 to 370 nm. The observed changes in the optical absorption spectra when the backbone structure is varied can be attributed to the modification of the polymer chain planarity [9] For monomer and polymer, λ_{onset} values regarding CBAAMP, P-CBAAMPXB, P-CBAAMPBD, P-CBAAMPCEE and P-CBAAMPBCEE were calculated as 420, 390, 370, 380 and 370 nm, respectively. E_g values were calculated from $1242/\lambda_{onset}$ and given in Table 3. The conjugation is disrupted due to the presence of high sterically hindered structures and E_g values of the polymers are observed greater than those of Schiff bases.

Electrochemical properties of some synthesized Schiff base monomers and the polymers were examined by using cyclic voltammetry (CV) technique and the oxidation–reduction peak potentials belonging to potential-current voltammograms of monomers and their polymers are given in Fig. 5 as coincident. While only one oxidation peak is observed in the positive region for both monomer and polymer in the spectrum, three peaks are observed in the negative region regarding the reduction of imine (—HC═N) nitrogen by being protonated. CVs of all monomers and polymers were taken by using glassy carbon electrode (GCE). The solution of $TBAPF_6$ in acetonitrile was used as the solvent. Electrochemical data of all compounds are given in Table 3. The lower band gaps facilitate the electronic transitions between HOMO and LUMO energy levels and make the polymers more electro-conductive than the monomers.

Fluorescence absorption spectrums of the synthesized compounds were taken at room temperature by using DMSO as the solvent. In all analyses, the emission and excitation slit range was set to 5 nm. The wavelengths of emission and excitation peaks for spectrums of the synthesized Schiff base and the polymers by using condensation method are given in Fig. 6. The conjugated substances emit light with different intensities by exhibiting fluorescence characteristics at different wavelengths. If the light emitted by a substance falls in the visible region of electromagnetic spectrum, the substance is found to have a visible colored emission. The color changes according to the wavelength of the light in electromagnetic spectrum are shown in Fig. 6. In the spectrum given in Fig. 6, the intensity and color of the light were observed to be better at 350 and

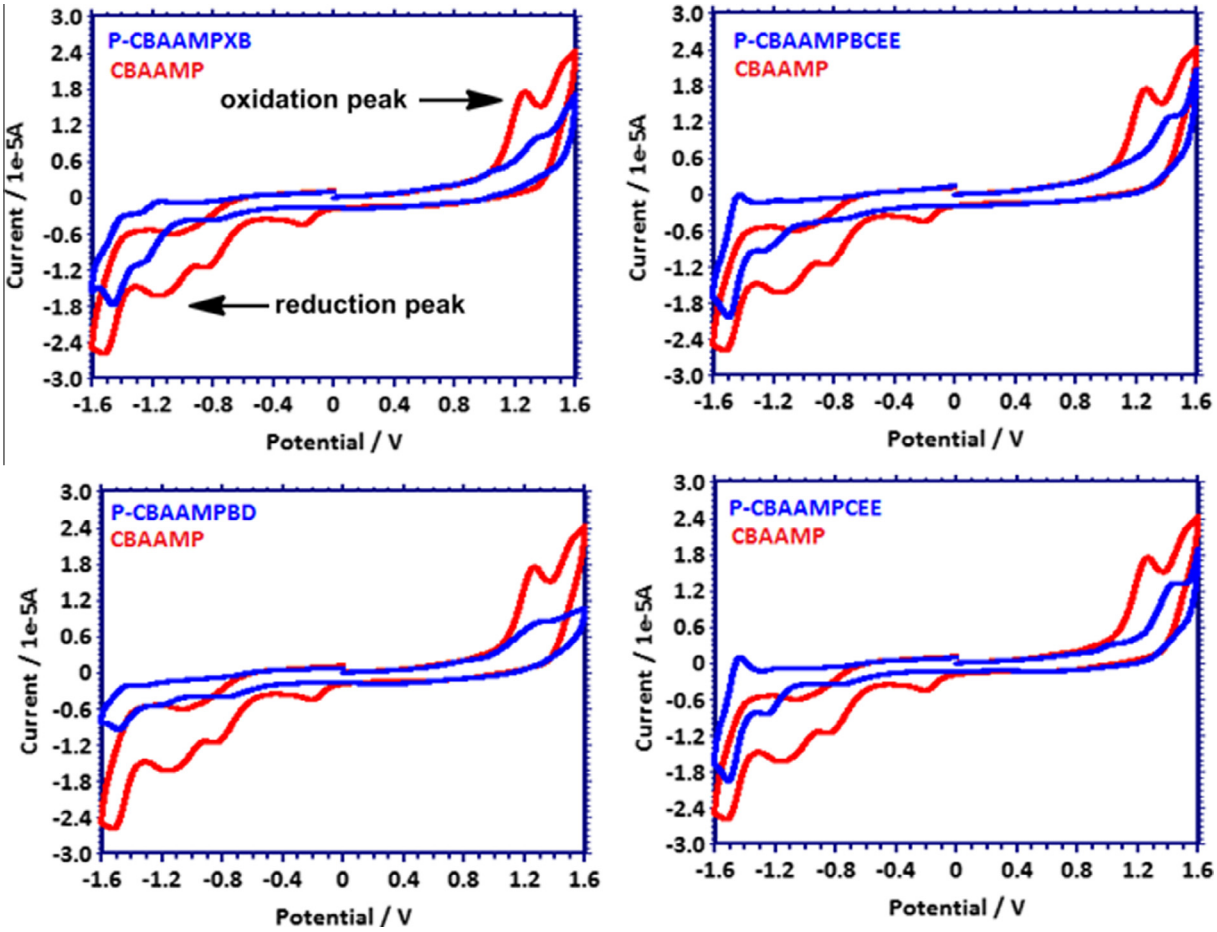

Figure 5 Cyclic voltammograms of the synthesized compounds.

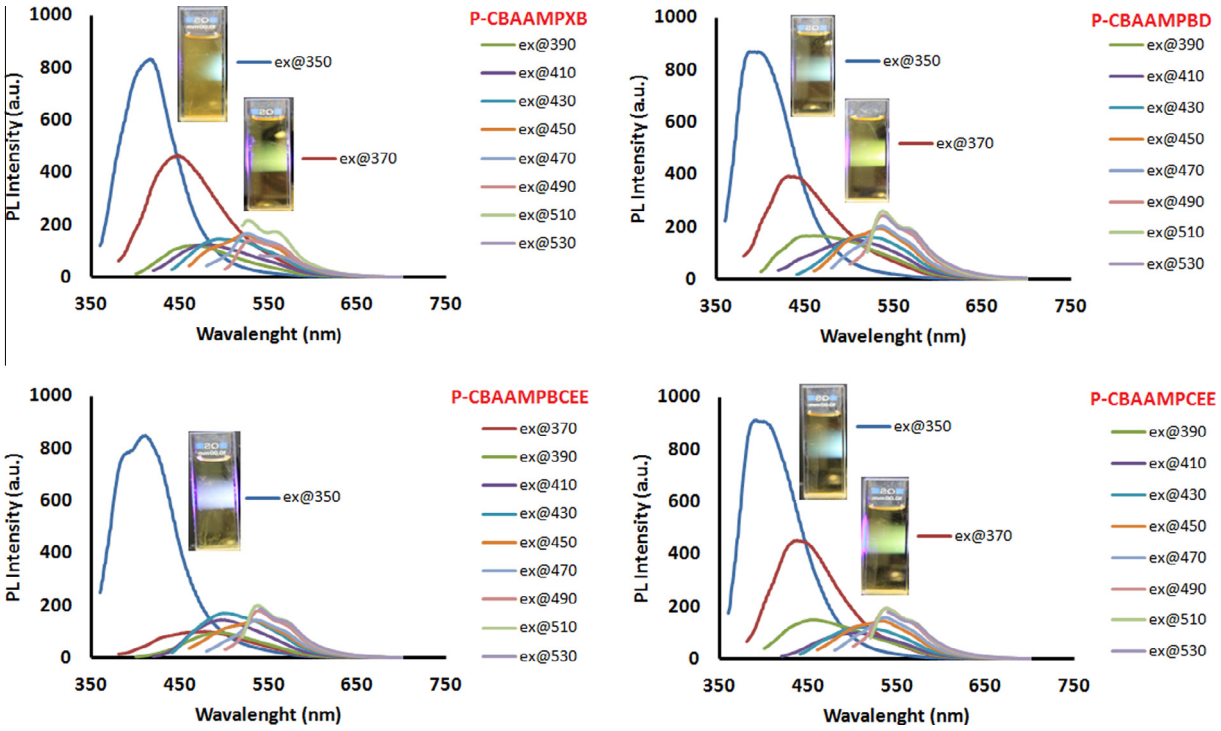

Figure 6 Emission spectra of solutions in THF Slit width: λ_{Ex} 5 nm, λ_{Em} 5 nm; concentration of the compounds: 0.01 mg/mL.

370 nm when the emission and intensity of the light was examined up to 530 nm by increasing 20 nm of intervals starting from the excitation at 350 nm. It was observed that as wavelength increased, the intensity of the light weakened and color was not seen. The maximum emission wavelength and the maximum emission intensity for each polymer are given in Table 4. The emission color can be stated regarding the substance due to the wavelength of the peak obtained in fluorescence spectrum.

3.2. Electrical conductivities

For polymers, the graph plotted versus time regarding to the solid state conductivity values measured at air atmosphere. The measurements for the polymers were carried out in pure form, and then polymers were exposed to iodine vapor in a desiccator, and the change in their conductivities versus time was measured at specific time intervals by doping. In doping process, electron emitting amine nitrogen and electron pulling iodine coordinate, and the formation of radical cation (polaron) structure in polymer chain (on amine nitrogen) are enabled. The electron vacancy formed due to this polaron facilitates the electron flow, and this causes electrical conductivity to increase. High electron intensity allows the polymer to coordinate with iodine more, and consequently an increase at a higher level for the electron flow is obtained. After 120 h doping, the conductivity of P-CBAAMPXB is observed around 10^{-7} S cm^{-1} and it is better than that of P-CBAAMPBD. For poly(azomethine)s, the conductivities of the undoped polymers were 10^{-11} S/cm, while those of the doped with iodine ones

Table 4 Fluorescence spectral data of the synthesized compounds with optimum concentrations in THF solvent.

Compounds	λ_{Ex}										
		350	370	390	410	430	450	470	490	510	530
P-CBAAMPXB	$\lambda_{max\ (Em)}$	415	446	460	482	505	522	525	528	527	563
	I_{Em}	831	464	119	129	142	159	167	143	213	77
P-CBAAMPBD	$\lambda_{max\ (Em)}$	393	435	462	505	518	534	536	537	537	537
	I_{Em}	869	393	164	150	160	194	204	246	262	141
P-CBAAMPCEE	$\lambda_{max\ (Em)}$	395	442	457	502	509	532	536	537	538	541
	I_{Em}	904	450	150	97	120	146	155	190	196	176
P-CBAAMPBCEE	$\lambda_{max\ (Em)}$	409	469	491	499	503	534	538	538	538	538
	I_{Em}	845	99	97	142	164	142	142	180	199	187

λ_{Ex}: excitation wavelength for emission, $\lambda_{max\ (Em)}$: maximum emission wavelength, I_{Em}: maximum emission intensity.

Table 5 Thermal degradation values of the synthesized compounds.

Compounds	[a]T_{on}	[b]$W_{max.}T$	20% Weight loss	50% Weight loss	% Char at 1000 °C	DTA exo/endo	DSC [c]T_g (°C)/[d]ΔC_p (J/g)
CBAAMP	242	267	254	285	10	–/265	–
P-CBAAMPXB	239	277, 355, 550	280	368	22	–/–	152/0.157
P-CBAAMPBD	354	390	330	392	25	–/–	139/0.099
P-CBAAMPCEE	280	316, 404	306	406	24	–/–	143/0.124
P-CBAAMPBCEE	285	328, 396	312	386	22	–/–	165/0.066

[a] The onset temperature.
[b] Maximum weight temperature.
[c] Glass Transition Temperature.
[d] Change of specific heat during glass transition.

were 10^{-9} S/cm. The low conductivity values were attributed to the low degree of conjugation in the polymers caused by non-planarity of the polymer chains [14–16]. At low temperatures, the conductivity of the poly(azomethine)s doped with I_2 was slightly higher than that of the undoped one. The conductivity of the doped polymer showed an abrupt increase in conductivity from 10^{-11} to 10^{-7} S/cm [16]. The conductivity of polyesters containing azomethine linkages was in the range 10^{-9} to 10^{-14} S/cm [17]. Poly(azomethine)s showed semiconductor behavior and the conductivity rapidly increases from 10^{-11} to

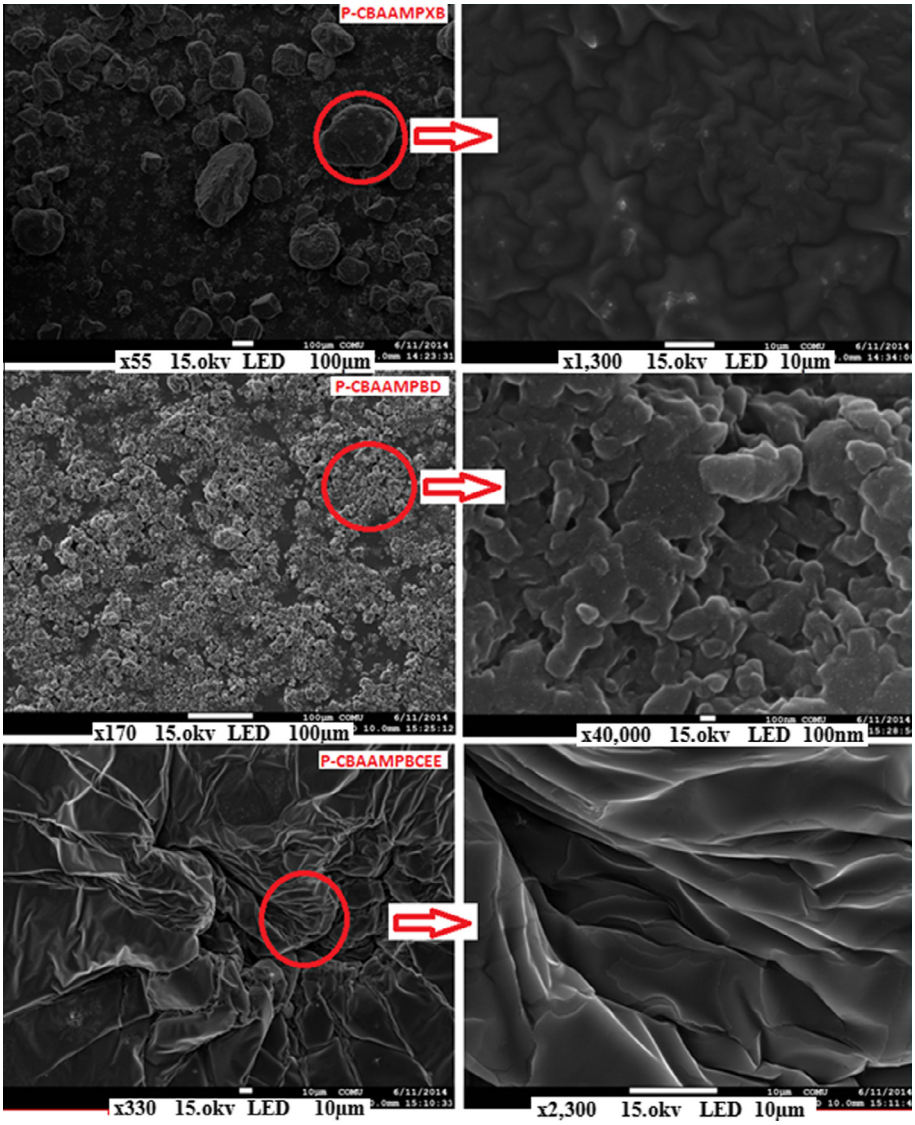

Figure 7 SEM photographs of P-CBAAMPXB, P-CBAAMPBD and P-CBAAMPBCEE.

10^{-7} S/cm. It is curious that a similar behavior was found for the polyazomethine doped with I_2 and H_2SO_4 at higher temperature than 80 °C [15].

3.3. Thermal analysis of compounds

TG measurements of polymers synthesized in 4 different structures by carrying out esterification reaction between 2-amino-5-methyl phenol and 4-hidroxybenzaldehyde Schiff base and various aliphatic and aromatic dihalogen compounds were determined in N_2 atmosphere at 1000 °C. TG and DSC thermograms taken to determine T_{20}, T_{50} and T_{on} temperatures and the number of decomposition steps, exothermic and endothermic peaks, glass transition temperatures (T_g) and specific heat change (ΔC_p) of monomers and the values measured from thermograms are shown in Table 5. According to Table 5, the initial decomposition temperatures of P-CBAAMPBD, P-CBAAMPCEE and P-CBAAMPBCEE are higher than those of the monomer. This is because of the formation of the C—O etheric bond during the OP reaction (C—O—C coupling). This weak bond is easily broken at moderate temperatures and makes the polymer thermally unstable [18]. It suggests that, both the polymers have good thermal stability as the starting weight loss for the polymers is situated within the 239–354 °C range [19]. The weight loss curve gives the degradation process in nitrogen and it presents two stages, one main weight loss ester link-age and in the second stage a —N═CH— group. When compared with a similar structure and high temperature it can be confirmed that the —N═CH— group is breaking at the second stage weight loss [20,21]. The presence of the aliphatic group in the structure increases the thermal stability. When initial decomposition temperatures (T_{on}) and glass transition temperatures (T_g) of the synthesized polymers are compared according to polymer types, the calculated glass transition temperatures are found to be below the initial decomposition temperature as expected. The glass transition temperatures of the polymers lie between 139 and 165 °C, as observed in DSC analysis. The high glass transition temperatures are attributed to the presence of the rigid structure along the main chain. Also the presence of intermolecular hydrogen bonding indicates a more amorphous structure [13]. In general, only the polyesters having a linear chain shape were semicrystalline and thermotropically liquid crystalline. For the polymer conformational adjustment arising from the flexible oxygen bridges C_{2V} symmetry of such a highly angled molecular arrangement certainly helps in the formation of a mesophase [22].

3.4. Morphological characterization

SEM images of surface morphologies for the synthesized Schiff base polymers are given in Fig. 7. In the image of P-CBAAMPXB at 100 μm and 10 μm, it was observed that it consists of particles which are similar to convolutions of brain cells and sizes of these particles were close to each other; as regards P-CBAAMPBD, it was observed that it contains flatter surfaces formed as a result of combination of particles and non-routine cracks and gaps. Since the structures of P-CBAAMPBCEE and P-CBAAMPCEE are similar, SEM image was taken and showed a similar structure like a flower. It was seen that it consists of smooth structures in layers when approached to the surface.

4. Conclusions

In this study, while P-CBAAMPXB and P-CBAAMPBD polymers were obtained in dark brown colored powder form, P-CBAAMPBCEE and P-CBAAMPCEE polymers with different carbon numbers and ether bridges were black color in viscous form. Conductivity measurement could not be carried out since these viscous polymers could not be pelletized but its solubility was found to be better due to etheric groups and yield of the polymers were lower than that of the others. Synthesized polymers showed good solubility because of the existence of ether linkages. Fine solubility of the synthesized polymer maximizes its practical applications. According to optical property of the synthesized polymers, optical band gap (E_g) and electro optical band gap (E'_g) values vary depending on the increase of conjugation and the electrical conductivity measurement by doping with iodine gave good results. The semi-conductive polymer was used in electronic, optoelectronic and photovoltaic applications. Abilities of the polymers to be used in gas sensing materials were discussed. When thermal analysis results of polymers were compared, maximum initial decomposition temperature was observed in 354 °C for P-CBAAMPBD due to the presence of aliphatic group. Consequently, because of the high thermal stabilities the synthesized compounds can be promising candidates for aerospace applications, and they can be used to produce temperature-stable materials.

Acknowledgements

The authors thank the Çanakkale Onsekiz Mart University scientific research project commission for support with the project number (Project No.: FBA-2013-115).

References

[1] İ. Kaya, M. Yıldırım, A. Avcı, Synthesis and characterization of fluorescent polyphenol species derived from methyl substituted aminopyridine based Schiff bases: the effect of substituent position on optical, electrical, electrochemical, and fluorescence properties, Synth. Metals 160 (2010) 911–920.
[2] İ. Kaya, M. Kamacı, Synthesis and characterization of new poly(azomethine-urethane) and polyphenol derivatives obtained from 3,4-dihydroxy benzaldehyde and hexamethylene diisocyanate, Polimery 56 (2011) 721–733.
[3] A. Sikora, A. Iwan, AFM study of the mechanical wear phenomena of the polyazomethine with thiophene rings: tapping mode, phase imaging mode and force spectroscopy, High Perform. Polym. 24 (2012) 218–228.
[4] A. Gul, Z. Akhter, A. Bhatti, A. Siddiq, A. Khan, H.M. Siddiqe, N.K. Janjua, A. Shaheen, S. Sarfraz, B. Mirza, Synthesis, physicochemical studies and potential applications of high-molecular-weight ferrocene-based poly(azomethine)ester and its soluble terpolymers, J. Organomet. Chem. 719 (2012) 41–53.
[5] P. Karimi, A.S. Rizkallanm, K. Mequanint, Versatile biodegradable poly(ester amide)s derived from α-amino acids for vascular tissue, Eng. Mater. 3 (2010) 2346–2368.
[6] J. Zuo, S. Li, L. Bouzidi, S.S. Narine, Thermoplastic polyester amides derived from oleic acid, Polymer 52 (2011) 4503–4516.
[7] K.R. Reddy, A.R. Raghu, H.M. Jeong, Synthesis and characterization of novel polyurethanes based on 4,4′-{1,4-phenylenebis[methylylidenenitrilo]} diphenol, Polym. Bull. 60 (2008) 609–616.

[8] W. He, Y.Y. Jianga, A.S. Luytc, R.O. Ocayad, T.J. Ge, Synthesis and degradation kinetics of a novel polyester containing bithiazole rings, Thermochim. Acta 525 (2011) 9–15.
[9] A. Iwan, M. Palewicza, A. Sikoraa, A. Chmielowieca, J. Hreniaka, A. Grzegorz Pasciaka, P. Bilski, Aliphatic–aromatic poly(azomethine)s with ester groups as thermotropic materials for opto(electronic) applications, Synth. Metals 160 (2010) 1856–1867.
[10] S. Çulhaoğlu, İ. Kaya, Synthesis, characterization, thermal stability and conductivity of new Schiff base polymer containing sulfur and oxygen bridges, Polymer (Korea) 39 (2015) 225–234.
[11] İ. Kaya, M. Yıldırım, M. Kamacı, Synthesis and characterization of new polyphenols derived from *o*-dianisidine: the effect of substituent on solubility, thermal stability, and electrical conductivity, optical and electrochemical properties, Eur. Polym. J. 45 (2009) 1586–1598.
[12] İ. Kaya, A. Bilici, Synthesis, characterization, thermal analysis, and band gap of oligo-2-methoxy-6-[(4-methylphenyl)imino]-methylphenol, J. Appl. Polym. Sci. 104 (2007) 3417–3426.
[13] C.H.R.M. Wilsens, Y.S. Deshmukh, B.A.J. Noordover, S. Rastogi, Influence of the 2,5-furandicarboxamide moiety on hydrogen bonding in aliphatic-aromatic poly(ester amide)s, Macromolecules 47 (2014) 6196–6206.
[14] S.C. Ng, H.S.O. Chan, P.M.L. Wong, K.L. Tan, B.T.G. Tan, Novel heteroarylene polyazomethines: their syntheses and characterizations, Polymer 39 (1998) 4963–4968.
[15] A.G. El-Shekeil, H.A. Al-Saady, F.A. Al-Yusufy, Synthesis and characterization of some soluble conducting polyazomethine polymers, New Polym. Mater. 5 (1998) 131–140.
[16] A.G. El-Shekeil, M.A. Khalid, F.A. Al-Yusufy, A comparative study of some undoped aromatic polyazomethines, Macromol. Chem. Phys. 202 (2001) 2971–2979.
[17] V.D. Bhatt, A. Ray, Synthesis, characterization and electrical conductivity of polyesters containing azomethine linkages, Int. J. Polym. Mater. 49 (2001) 355–366.
[18] İ. Kaya, M. Yıldırım, A. Aydın, D. Şenol, Synthesis and characterization of fluorescent graft fluorene-co-polyphenol derivatives: the effect of substituent on solubility, thermal stability, conductivity, optical and electrochemical properties, React. Funct. Polym. 70 (2010) 815–826.
[19] B. Joy Vasanthi, L. Ravikumar, Synthesis and characterization of poly(azomethine ester)s with a pendent dimethoxybenzylidene group, Open J. Polym. Chem. 3 (2013) 70–77.
[20] Y. Saegusa, K. Sekiba, S. Nakamura, Synthesis and characterization of novel 1,3,4-oxadiazole- or 1,3,4-thiadiazole-containing wholly conjugated polyazomethines, J. Appl. Polym. Sci. Part A: Polym. Chem. 28 (1990) 3647–3659.
[21] M. Grigoras, N.C. Antonoaia, Synthesis and characterization of some carbazole-based imine polymers, Eur. Polym. J. 41 (2005) 1079–1089.
[22] E.J. Choi, B.K. Choi, J.H. Kim, S.C. Lee, D.J.T. Hill, Synthesis and properties of oxygen-bridged aromatic polyesters based on isomeric naphthalenediols, Korea Polm. J. 8 (2000) 12–18.

Please cite this article in press as: D. Şenol, İ. Kaya, Synthesis and characterization of azomethine polymers containing ether and ester groups, Journal of Saudi Chemical Society (2015), http://dx.doi.org/10.1016/j.jscs.2015.05.006